Microbial Cell Factories

RESEARCH

Open Access

Engineering the secretome of *Aspergillus niger* for cellooligosaccharides production from plant biomass

Fernanda Lopes de Figueiredo[1†], Fabiano Jares Contesini[1,2†], César Rafael Fanchini Terrasan[1], Jaqueline Aline Gerhardt[1], Ana Beatriz Corrêa[1], Everton Paschoal Antoniel[1], Natália Sayuri Wassano[1], Lucas Levassor[2], Sarita Cândida Rabelo[3], Telma Teixeira Franco[4], Uffe Hasbro Mortensen[2] and André Damasio[1*]

Abstract

Background Fermentation of sugars derived from plant biomass feedstock is crucial for sustainability. Hence, utilizing customized enzymatic cocktails to obtain oligosaccharides instead of monomers is an alternative fermentation strategy to produce prebiotics, cosmetics, and biofuels. This study developed an engineered strain of *Aspergillus niger* producing a tailored cellulolytic cocktail capable of partially degrading sugarcane straw to yield cellooligosaccharides.

Results The *A. niger prtT*Δ strain created resulted in a reduced extracellular protease production. The *prtT*Δ background was then used to create strains by deleting exoenzyme encoding genes involved in mono- or disaccharide formation. Consequently, we successfully generated a tailored *prtT*Δ*bglA*Δ strain by eliminating a beta-glucosidase (*bglA*) gene and subsequently deleted two cellobiohydrolases and one beta-xylosidase encoding genes using a multiplex strategy, resulting in the *Quintuple*Δ strain (*prtT*Δ; *bglA*Δ; *cbhA*Δ; *cbhB*Δ; *xlnD*Δ). When applied for sugarcane biomass degradation, the tailored secretomes produced by *A. niger* resulted in a higher ratio of cellobiose and cellotriose compared with glucose relative to the reference strain. Mass spectrometry revealed that the *Quintuple*Δ strain secreted alternative cellobiohydrolases and beta-glucosidases to compensate for the absence of major cellulases. Enzymes targeting minor polysaccharides in plant biomass were also upregulated in this tailored strain.

Conclusion Tailored secretome use increased COS/glucose ratio during sugarcane biomass degradation showing that deleting some enzymatic components is an effective approach for producing customized enzymatic cocktails. Our findings highlight the plasticity of fungal genomes as enzymes that target minor components of plant cell walls, and alternative cellulases were produced by the mutant strain. Despite deletion of important secretome components, fungal growth was maintained in plant biomass.

Keywords *Aspergillus niger*, CAZymes, Cellooligosaccharides, Fungal engineering, Tailor-made enzymatic cocktail, Sugarcane biomass

†Fernanda Lopes de Figueiredo and Fabiano Jares Contesini share the first authorship.

*Correspondence:
André Damasio
adamasio@unicamp.br
Full list of author information is available at the end of the article

Background

The negative impacts of fossil fuels on the climate and environment demand a change towards plant biomass-derived products in biorefineries [1–4]. In biorefineries, plant biomass is converted (refined) into relevant products or energy [5–7]. Traditionally, plant biomass components such as cellulose and hemicellulose are degraded into monosaccharides by efficient enzyme cocktails produced by microbial cell factories. Monosaccharides are then used to feed other microbial cell factories, e.g., *Saccharomyces cerevisiae* [8–10]. Recently, an efficient and cost-effective alternative approach suggests using oligosaccharides derived from partially degraded lignocellulosic material instead of monosaccharides for fermentation [10, 11]. This new strategy offers numerous advantages. First, fewer enzymes are needed for the saccharification process. Second, it introduces a novel path in synthetic biology and metabolic engineering for constructing fermentative strains with advantageous features for large-scale bioreactors [12–14]. Finally, oligosaccharides are resistant to compression, retain oils, and form powders with high fluidity, which can improve formulation processes for prebiotics, food supplements and medicine production [13–18]. Using oligosaccharides could reduce contamination risks during fermentation because only fungi, and not bacteria, can transport and consume the oligosaccharides [19–21]. Cellulose and hemicellulose are the two primary polysaccharides found in plant cell walls. Xylooligosaccharides (XOS) can be highly produced from hemicellulose through a previously described hydrothermal and deacetylation pretreatment [22], in which cellulose constitutes the predominating solid fraction, necessitating tailored enzymatic cocktails for conversion into cellooligosaccharides (COS) [23].

Some characteristics and functional properties of COS are relevant to industrial applications. The health sector focuses on their prebiotic function in the large intestine, where COS is an ideal substrate for beneficial microorganisms. COS resists the initial stages of digestion and can, therefore, be easily incorporated into feed formulations and used as a supplement in diets [24–27]. Additionally, there is a growing interest in using short-chain COS (cellobiose and cellotriose) as prebiotics. COS is the main substrate for the in vitro growth of intestinal bacteria strains such as *Lactobacilli* and *Bifidobacteria* [18]. Studies on upscaling its production and evaluating prebiotic properties are scarce. Hence, further research and analysis are necessary to address this issue [13, 28, 29].

Cellulose degradation is performed by glycoside hydrolases (GHs) and oxidative enzymes classified in the auxiliary activity class (AAs) [24]. Initially, endoglucanases (EGLs) randomly cleave beta-1,4 glycosidic bonds, forming shorter cellulose chains and COS with different degrees of polymerization depending on the reaction time. The EGL-derived products are then cleaved by cellobiohydrolases (CBHs) that bind to the cellulose chains via their funnel-like active site to release cellobiose as a main product. Lytic polysaccharide monooxygenases (LPMOs) from family AA9 acting on crystalline cellulose turns the polymer more accessible to EGLs and CBHs [27] and contributes to COS production in long-term reactions [25]. At the end of the process, cellobiose and other COS are degraded into glucose molecules by beta-glucosidases (BGLs) [28].

Due to high efficiency in protein production, Aspergilli is one of the most used microbial cell factories in biotechnology [23, 26, 30, 31]. Within this genus, *Aspergillus niger* is an industrial workhorse and one of the main representative species that has been studied over the decades for enzyme production due to its efficient secretory pathway [32]. Given such interest, an elaborate genetic toolbox has been developed, including efficient CRISPR technologies for gene deletion, gene insertion, and site-directed mutagenesis [10, 33, 34]. This is important as genetic modifications of *Aspergillus* spp. are needed to meet the requirements of industrial applications. Common approaches to developing fungal platforms include deleting morphological genes, such as *racA* [35], chaperone deletion [36], upregulating cofactor metabolism [37], as well as deleting amylase [38] and protease regulators [39]. Similarly, strain engineering can be employed to create robust *A. niger* enzyme producers, along with designing optimized enzymatic cocktails for plant biomass degradation [11, 23, 28, 40].

In this study, we investigated the potential of *A. niger* as a source for a customized cellulolytic cocktail that can efficiently produce COS from sugarcane straw. For this purpose, we deleted critical exoenzyme-encoding genes found in a previously published *A. niger* secretome produced in sugarcane bagasse [41]. Absence of the main BGLs and CBHs in the secretome of the mutant strain resulted in a significantly higher COS/glucose ratio derived from plant biomass degradation. These findings provide important insights into how targeted genetic deletions can contribute to optimizing cellulolytic enzyme mixtures for COS production from agricultural waste such as sugarcane straw.

Materials and methods

Strains and cultivation media

Aspergillus niger ATCC1015 (*pyrG1*, *kusA*Δ) [34] was used to generate all strains described in this study (Additional Table 1). The strains were maintained on minimal medium (MM) composed of 1×Clutterbuck's salts (20×Clutterbuck's salts stock: 1.4 M $NaNO_3$, 0.13 M KCl, 0.042 M $MgSO_4{\cdot}7H_2O$ and 0.22 M KH_2PO_4),

1×trace elements (1000×Trace elements stock: 7.2 mM $ZnSO_4{\cdot}7H_20$, 17.7 mM H_3BO_3, 2.52 mM $MnCl_2{\cdot}4H_20$, 2.72 mM $FeSO_4{\cdot}7H_20$, 0.95 mM $CoCl_2{\cdot}5H20$, 0.7 mM $CuS0_4{\cdot}5H_20$, 0.21 mM $Na_2Mo0_4{\cdot}4H_20$ and 17.11 mM EDTA), 5 mM uracil and 5 mM uridine (u/u), pH 5.5, supplemented with 1% (w/v) glucose (Sigma-Aldrich) and maintained at 30 °C. *Escherichia coli* DH5α was cultivated in Luria Bertani (LB) (Sigma-Aldrich) media and used to propagate all plasmids.

DNA manipulation and gene deletions

Genomic DNA from *A. niger* strains were isolated using FastDNA SPIN for Soil DNA extraction kit (MP Biomedicals, USA). Primers were designed using *A. niger* genome sequences for the following genes: extracellular protease regulator (*prtT*—ID ASPNIDRAFT2_1146707), cellobiohydrolase B (*cbhB* – GH7 – ID ASPNIDRAFT2_1117716), cellobiohydrolase A (*cbhA* – GH 7—ID ASPNIDRAFT2_1164625, beta-glucosidase (*bglA* – GH3—ID ASPNIDRAFT2_1147525), beta-xylosidase (*xInD* – GH3- ID ASPNIDRAFT2_1156695) and other six beta-glucosidases (GH3s – IDs – ASPNIDRAFT2_1099883, ASPNIDRAFT2_1105418, ASPNIDRAFT2_1126962, ASPNIDRAFT2_1157877, ASPNIDRAFT2_37673 and ASPNIDRAFT2_1173382) publicly available in FungiDB (version 5.0) and JGI (version 4.0), respectively [42, 43] (Additional Fig. 1 and Additional Tables 1 and 2). DNA fragments were amplified by touch-down PCR with annealing temperature ranging from 68–50.5 °C in 35 cycles using proofreading PfuX7 polymerase [44] or Phusion U (Thermofisher). PCR reactions were prepared in 50 µL including 1×Phusion HF Buffer (New England Biolabs, USA), 0.4 µM primers (TAG Copenhagen, Denmark), 0.2 mm dNTPs, 1 U PfuX7, 1–50 gDNA/plasmid as template, 3% DMSO (Additional Fig. 1). All vectors were constructed by USER cloning [45] using plasmid backbones previously described [46, 47]. Specific information for constructing CRISPR vectors containing tRNAs based on in vivo sgRNA release was described in a previous study [46] (Additional Table 2). All vectors assembled to construct the tailored strains are listed in Additional Table 1.

Fungal transformation

A. niger transformation was performed as previously described [48]. Approximately 2 µg of CRISPR vectors and 10 µL of single-stranded oligonucleotides (GE Life Science) solution (100 µM) were used for gene editing. Diagnostic PCR was performed using fungal mycelia or extracted genomic DNA using primers annealing to 200 – 300 base pairs (bp) upstream and downstream regions of the deleted ORF. Primers and repairing oligonucleotide sequences are listed in Additional Table 2.

Protein analysis

Protein concentration in the fungal secretomes was quantified using the BCA method (Thermo Scientific). The secretome profiles (20 µg protein) were visualized in 12% SDS-PAGE stained with Coomassie Brilliant blue R-250 [49].

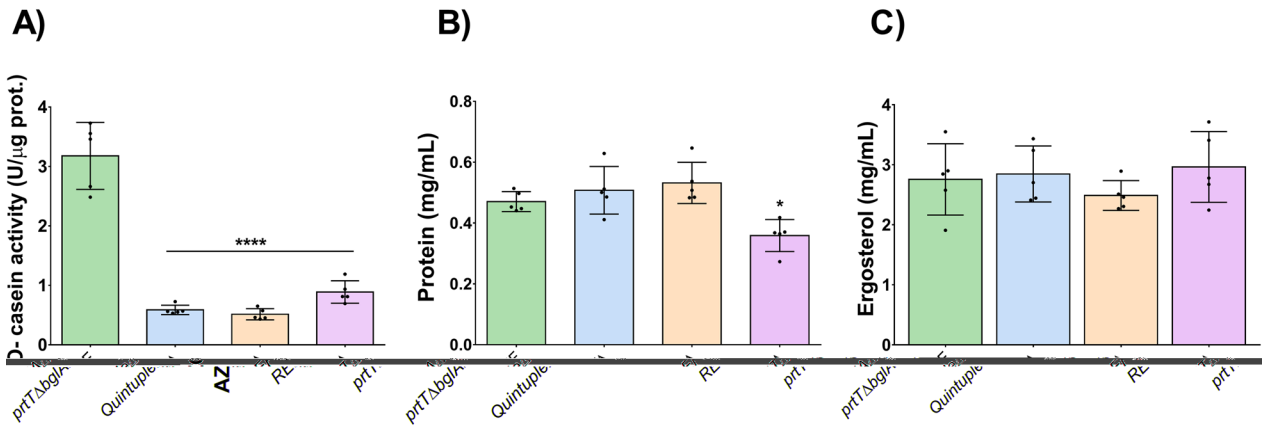

Fig. 1 Analysis of protease activity, protein secretion, and fungal growth of the tailored strains. **A** Proteolytic activity (U/µg prot.) in the secretomes using AZO-casein (5 mg/mL) as substrate. **B** Protein amount (mg/mL) in the secretomes. **C** Indirect analysis of fungal growth measured by quantification of mycelial ergosterol (mg/mL). Secretomes and mycelia were obtained from cultures containing 1×10^6 spores/mL inoculated in liquid medium supplemented with 1% (w/v) SCB for 72 h at 30 °C and 180 rpm. Cultivation was conducted in five replicates. Statistical analysis was performed using multiple tests (two-factor ANOVA with Tukey's test—p-value ≤ 0.05) in comparison with the *REF* strain as follows: $*p < 0.05$, $**p < 0.01$, $***p < 0.001$

Phenotyping of the tailored strains

Growth on different substrates

Conidia suspensions of each strain were inoculated (1×10^5 conidia/mL final concentration) on the center of MM Petri dishes (as described above), supplemented with 1% (w/v) of glucose, microcrystalline cellulose (Avicel) (Sigma-Aldrich), carboxymethyl cellulose (CMC) (Sigma-Aldrich), hydrothermally and deacetylated pretreated sugarcane bagasse (SCB), xylose (Sigma-Aldrich), and xylan from beechwood (Sigma-Aldrich). Assay was performed in five replicates at 30 °C for 7 days.

Cultivation in liquid medium

Conidia suspensions were inoculated (1×10^6 conidia/mL final concentration) on Erlenmeyer flasks (250 mL) containing 50 mL of liquid MM u/u 2% glucose (w/v) pH 5.5 for 24 h at 30 °C for pre-cultivation. After 24 h, mycelia were removed by filtration, abundantly washed with distilled water, and transferred to Erlenmeyer flasks (250 mL) containing 50 mL of liquid MM u/u pH 5.5 supplemented with 1% SCB or glucose for 72 h at 30 °C. Subsequently, mycelia were removed by filtration, and the secretome was concentrated using 10 kilodaltons (kDa) cutoff Amicon (Merck) for protein quantification, SDS-PAGE analysis, and enzymatic and saccharification assays.

Ergosterol extraction and quantification

Solid fractions containing mixtures of mycelium and biomass from SCB cultures were used for ergosterol extraction [50]. The assay was performed in five replicates. After extraction, samples were diluted and analyzed in a High-Performance Liquid Chromatography (HPLC) system equipped with an absorbance A_{280} detector coupled to a C18 reversed-phase column (Supelco, 25 cm × 4.6 mm, 10 mm) and isocratically eluted with 1 mL/min methanol. Total ergosterol was quantified based on peak area using standard ergosterol (Sigma-Aldrich).

Enzyme activity assays

Enzymatic activities in the secretomes were assayed using the following substrates: 5 mM 4-nitrophenyl β-D-cellobioside (pNPC) (Sigma-Aldrich), 4-nitrophenyl β-D-glucopyranoside (pNPG) (Sigma-Aldrich), 4-nitrophenyl β-D-xylopyranoside (pNPX) (Sigma-Aldrich)1% (w/v), 5% AZO-casein (Sigma-Aldrich) and 0.5% (w/v) CMC, xylan from beechwood and beta-glucan from barley (Megazyme). Filter paper activity (FPAse) assays were performed as previously described [51]. Reactions were performed with 40—400 µL from the secretomes in 1 M sodium phosphate buffer pH 6.0 at 50 °C during 0.5–1 h. AZO-casein assays followed standard protocol (Sigma-Aldich) with modifications (16 h and 37 °C). Reactions with polymeric substrates were interrupted with 100 µL of DNS and the released reducing sugars were measured at 540 nm (nm) [52]. Reactions using synthetic substrates were interrupted with 100 µL of 1 M sodium bicarbonate and the released 4-nitrophenolate was measured at 405 nm. AZO-casein assays were measured at 440 nm. All assays were performed in five replicates. One enzyme unit (U) corresponds to the amount of enzyme that catalyzes the conversion of one µmol of substrate per minute under assay conditions.

PASC and lignocellulose saccharification assays

Phosphoric acid-swollen cellulose (PASC) was prepared from Avicel PH-101 (Sigma-Aldrich) [53]. The optimized hydrothermally and deacetylated pretreated SCB and sugarcane straw (SCS) conditions were previously established [22]. The SCS was composed of 52.82% ± 0.81 of cellulose, 13.19% ± 0.23 of hemicellulose, 22.29% ± 0.16 of lignin, and 9.55% ± 0.20 of ashes. Reactions containing 0.5% PASC (w/v) were performed in five replicates with 0.02 mg protein from the secretomes in 0.3 mL of 50 mM sodium acetate buffer pH 5.0 and shaken in a Thermomixer (Eppendorf) at 50 °C, 1000 rpm for 24 h. Reactions containing 2% (w/v) of SCS were performed in four replicates with 0.5 (mg) total secretome in 1 mL for 72 h. Samples were cooled, centrifuged (13,500 rpm, 10 min), filtered (0.45 µm), and diluted. Their products were quantified using High-Performance Anion-Exchange Chromatography with Pulsed Amperometric Detection (HPAEC-PAD). Control assays corresponded to reactions without fungal secretomes. Commercial enzymatic cocktail (Celluclast, Novozymes) was used as the reference reaction. The protein amount applied for SCS assays was equivalent to 15 FPU/g Celluclast.

HPAEC-PAD analysis

Detection of oligosaccharides

Oligosaccharides released from reactions with PASC and SCS were quantified by HPAEC-PAD on a Dionex ICS6000 system (Thermo Fisher Scientific) equipped with a CarboPac PA 200 column (250 mm × 3 mm) (Thermo Fisher Scientific), as previously described [54]. Spectrum intensity (V) was calculated using established standard values of cellobiose, xylobiose, cellotriose, xylotriose, cellotetraose, xylotetraose, cellopentaose, xylopentaose, cellohexaose and xylohexaose. Chromatogram peaks were analyzed using the Chromeleon7 software version 7.2.5.9507 (Thermo Fisher Scientific).

Detection of monosaccharides

Glucose, xylose, and arabinose release were quantified by HPAEC on a Dionex ICS6000 system (Thermo Fisher Scientific) equipped with a CarboPac PA 1 column (250 mm

× 2 mm) (Thermo Fisher Scientific), and Pulsed Amperometric Detection (PAD) with a mobile phase composed of 30 mM sodium hydroxide (NaOH) at 30 °C for 30 min. The flow rate was 0.25 mL/min, and the injection volume was 10 µL. Spectrum intensity (V) was calculated using established standard values. Chromatogram peaks were analyzed using the Chromeleon7 software version 7.2.5.9507 (Thermo Fisher Scientific).

Mass balance and conversion calculations

Biomass balance and conversion were calculated using the following equations:

$$\begin{aligned} Glucan\ conversion\ (\%) = [((&(0.99 \times C\ glucose) + (0.95 \times C\ cellobiose) \\ &+ (0.96 \times C\ cellotriose) \\ &+ (0.83 \times C\ gluconic\ acid)] \times V]))/Mc)] \\ &\times 100 \end{aligned} \quad (1)$$

$$\begin{aligned} Xylan\ conversion\ (\%) = [((&(0.88 \times C\ xylose) \\ &+ (0.88 \times C\ arabinose) \\ &+ (0.72 \times\ C\ acetic\ acid) \\ &+ (0.94 \times\ C\ xylobiose] \times V]))/Mh)] \\ &\times 100 \end{aligned} \quad (2)$$

$$C = concentration;\ V = volume;$$
$$Mc = cellulosemass;\ Mh = hemicellulosemass$$

Secretome analysis by mass spectrometry

Triplicates of *prtT*Δ, *prtT*Δ*bglA*Δ, and *Quintuple*Δ strains secretome were filtered, centrifuged (13,000*g*, 20 min, 4 °C), and concentrated using 10-kDa cut-off Amicon Centrifugal Filter Units (Millipore). Protein concentration was measured using the BCA method (Thermo Scientific). Then, 20 µg of each secretome was partially resolved on 12% SDS-PAGE [49], excised from the gel, reduced, and digested with 20 mg/mL trypsin (Promega). After extraction, samples were dried under vacuum, and peptide mixtures were loaded onto a 2 cm C18 trap column (Thermo Fisher Scientific), which was connected in-line to a 15 cm C18 reverse-phase analytical column Thermo EasySpray ES803 (Thermo Fisher Scientific). Separation was performed using 100% Buffer A (0.1% formic acid in water) at 750 bar on the Thermo EasyLC 120 HPLC system (Thermo Fisher Scientific). The column oven was set at 45 °C to maintain optimal temperature conditions during analysis.

Peptides were eluted using a 45-min gradient, starting from 6 to 60% Buffer B (80% acetonitrile, 1% formic acid) at 250 nl/min flow rate. Q-Exactive (Thermo Fisher Scientific) was operated using a DD-MS2 top10 method. Full MS spectra were collected at 70,000 resolution with a 3×10^6 AGC target or 20 ms maximum injection time, covering a 300–175 m/z scan range. MS2 spectra were obtained at 17,500 resolution with a 1×10^6 AGC target value or 60 ms maximum injection time. A normalized collision energy of 25 was used with an intensity threshold set to 1.7e4. Dynamic exclusion was set to 60 s and ions with a charge state < 2 or unknown were excluded. MS performance and chromatography were monitored for consistency by running complex cell lysate quality control standards.

Raw files were analyzed using Proteome Discoverer 2.4. Label-free quantification (LFQ) was performed in the processing and consensus steps, and spectra were matched against the FungiDB database [55]. Dynamic modifications were set as Oxidation (M), GlcNac (N) and Acetyl on proteins N-termini. Cysteine carbamidomethyl was set as a static modification. All results were filtered at 1% FDR, and protein quantification was conducted using the built-in Minora Feature Detector. Spectra data were annotated according to *A. niger* ATCC1015 genome deposited on the Fungal and Oomycete Informatics Resources (https://fungidb.org/fungidb/app/). Differentially secreted proteins were identified according to their spectra counting using average spectra outputs, and quantitative values were applied to normalize the counts. Statistical analysis of the spectra used t-test (p-value ≤ 0.05) and log twofold change ≥ 1 ou ≤ −1, with data from the *A. niger prtTΔ* strain. Parameters used to run BLASTp (https://blast.ncbi.nlm.nih.gov/Blast.cgi) were E-value ≤ 40%, identity ≥ 40%, and consultation coverage ≥ 80%. Classification of Carbohydrate-Active Enzymes (CAZymes) and Carbohydrate-Binding Modules (CBM) was performed on dbCAN v.3 (www.csbl.bmb.uga.edu/ dbCAN2) and CAZy database (www.cazy.org/). Prediction of signal peptide (SP) and non-classical protein secretion was verified using SignalP 4.1 (www.cbs.dtu.dk/services/SignalP). Protein families were classified according to the Pfam database (https://pfam.xfam.org). After statistical analysis, selected protein amino acid sequences were collected from annotated genome sequences from the FungiDB and BLASTp databases.

Results and discussion

A tailored *A. niger* secretome degrades plant biomass into products with a higher COS/glucose ratio

Extracellular proteases are key contributors to the instability of enzyme cocktails [39, 56]. Transcriptional activator *prtT*, which plays an essential role in regulating the expression of several extracellular proteases, was then deleted [10, 57] (Additional Fig. 1A). This strategy was previously applied to maintain the stability of a heterologous cutinase in *A. niger* [39]. The secretome of a purified *prtT*Δ strain cultivated in the presence of SCB showed

approximately 80% reduction (from 3.18 to 0.63 U/μg) in extracellular protease activity compared with the *Reference* strain (*REF*) (Fig. 1A).

Based on the classical model of cellulose degradation (EGLs, CBHs, and BGLs), we hypothesized that reducing the activity of exoenzymes (CBHs and BGLs) could lead to a higher COS yield from SCS using tailored strains secretomes. We chose to delete genes encoding highly secreted cellobiohydrolase A (*cbhA*), cellobiohydrolase B (*cbhB*), and beta-glucosidase (*bglA*) based on a previous study on the *A. niger* secretome produced on sugarcane bagasse [41]. Additionally, a highly secreted beta-xylosidase (*xlnD*) was also deleted to prevent the production of xylose by degrading the residual hemicellulose present in SCS (approximately 13%) [22].

The genes selected were deleted in the *prtTΔ* background strain (Additional Figs. 1A–C, details in Additional Tables 1 and 2). Initially, we deleted the most abundantly secreted CBH (*cbhB*), followed by the simultaneous deletion of *cbhA*, *bglA*, and *xlnD*, resulting in a *QuintupleΔ* strain, considering the previous *prtT* deletion (Additional Fig. 1B and Additional Tables 1 and 2). Since CBHs are extensively secreted by filamentous fungi and contribute to fungal growth and plant biomass degradation [57, 58], we also constructed a double mutant by deleting only *bglA* in the *prtTΔ* background (*prtTΔbglAΔ*) (Additional Fig. 1C Additional Tables 1 and 2).

We assessed the radial growth of mutant strains in a minimal medium supplemented with various carbon sources. The tailored strains were capable of growing on the selected carbon sources and exhibited similar growth rates on monosaccharides such as glucose and xylose. However, the *Quintuple*Δ strain showed reduced growth on xylan (Additional Fig. 2A). Secretome analysis of the *Quintuple*Δ strain also revealed distinct changes in protein secretion. A qualitative analysis using SDS-PAGE showed the absence of a band at approximately 70–80 kDa (Additional Fig. 2B). Furthermore, we noticed the absence of bands around 30, 25, and 15 kDa (Additional Fig. 2B). Secretion profiles were consistent across all biological replicates (Additional Fig. 2B).

Subsequently, we evaluated the protein production, fungal growth, and enzymatic activity of the secretomes generated by customized strains on SCB. Deleting the *prtT* and *bglA* genes had no impact on protein secretion levels, whereas the *Quintuple*Δ strain showed a 24% decrease in protein secretion compared with the *REF* strain (from approximately 0.47 to 0.36 mg/mL) (Fig. 1B). These deletions did not adversely affect the growth of the mutant strains on SCB, as evidenced by fungal mycelia ergosterol quantification (Fig. 1C), indicating that these mutations did not compromise their use as a platform for enzyme production. Moreover, there was no significant difference in protease activity between *prtT*Δ, *prtT*Δ*bglA*Δ, and *Quintuple*Δ strains (Fig. 1A).

In addition to protein secretion and fungal growth, we evaluated enzymatic activities on different substrates. The *prtT*Δ*bglA*Δ and *Quintuple*Δ secretomes showed a considerable decrease of at least 50% in activity on pNPG (from approximately 0.49 to 0.23 U/mg) and 36% on CMC (from 0.11 to 0.07 U/mg). *Quintuple*Δ presented a reduction of approximately 80% in pNPC (from 0.18 to 0.04 U/mg) (Fig. 2A–D). Secretome of the tailored strains exhibited lower activity on beta-glucan, especially the *Quintuple*Δ secretome, showing only 10% of total activity (from 0.99 to 0.09 U/mg) (Fig. 2E). A 43% reduction (from 1 to 0.57 U/mg) in xylan activity was also observed in the *Quintuple*Δ secretome (Fig. 2F), corroborating the phenotypic analysis (Additional Fig. 2A). However, similar activity was observed for all strains on filter paper (Fig. 2G), suggesting that cellulase (Figs. 2B, D and E) and xylanase activities (Fig. 2C and F) depend on CBHs and beta-xylosidase XlnD, respectively. Moreover, BglA is responsible for about half of the total BGL activity in the secretomes (Fig. 2A).

Despite presenting lower protease secretion, the *prtT*Δ strain showed no significant differences in fungal growth, protein secretion, and enzymatic activities compared with the *REF* strain. Further experiments were conducted using the mutant strains *prtT*Δ*bglA*Δ and *Quintuple*Δ, and *prtT*Δ as reference. First, we evaluated PASC breakdown using secretomes produced by the tailored strains, which revealed that their secretomes exhibited similar product profiles characterized by reduced glucose production and comparable levels of cellotriose (Fig. 3A). Analyzing the sum of the products released (glucose, cellobiose and cellotriose), we found that the secretome produced by the *prtT*Δ*bglA*Δ strain showed increased levels of cellobiose. In contrast, the secretome of the *Quintuple*Δ strain exhibited lower amounts of cellobiose and glucose (Fig. 3A). Although both mutant strains had a higher COS/glucose ratio, the sum of products released was reduced. Specifically, the *Quintuple*Δ secretome yielded approximately 0.3 g/L, while the *prtT*Δ*bglA*Δ and *prtT*Δ strains yielded 0.6 g/L and 0.7 g/L respectively (Fig. 3A).

The same secretomes were applied to SCS saccharification. Commercial cocktail Celluclast was used as an internal control due to the lack of BGLs in its composition [59], similar to *prtT*Δ*blA*Δ and *Quintuple*Δ strains. The *Quintuple*Δ secretome released higher amounts of COS (approximately 1.51 g/L) and lower glucose concentration (approximately 0.03 g/L) compared

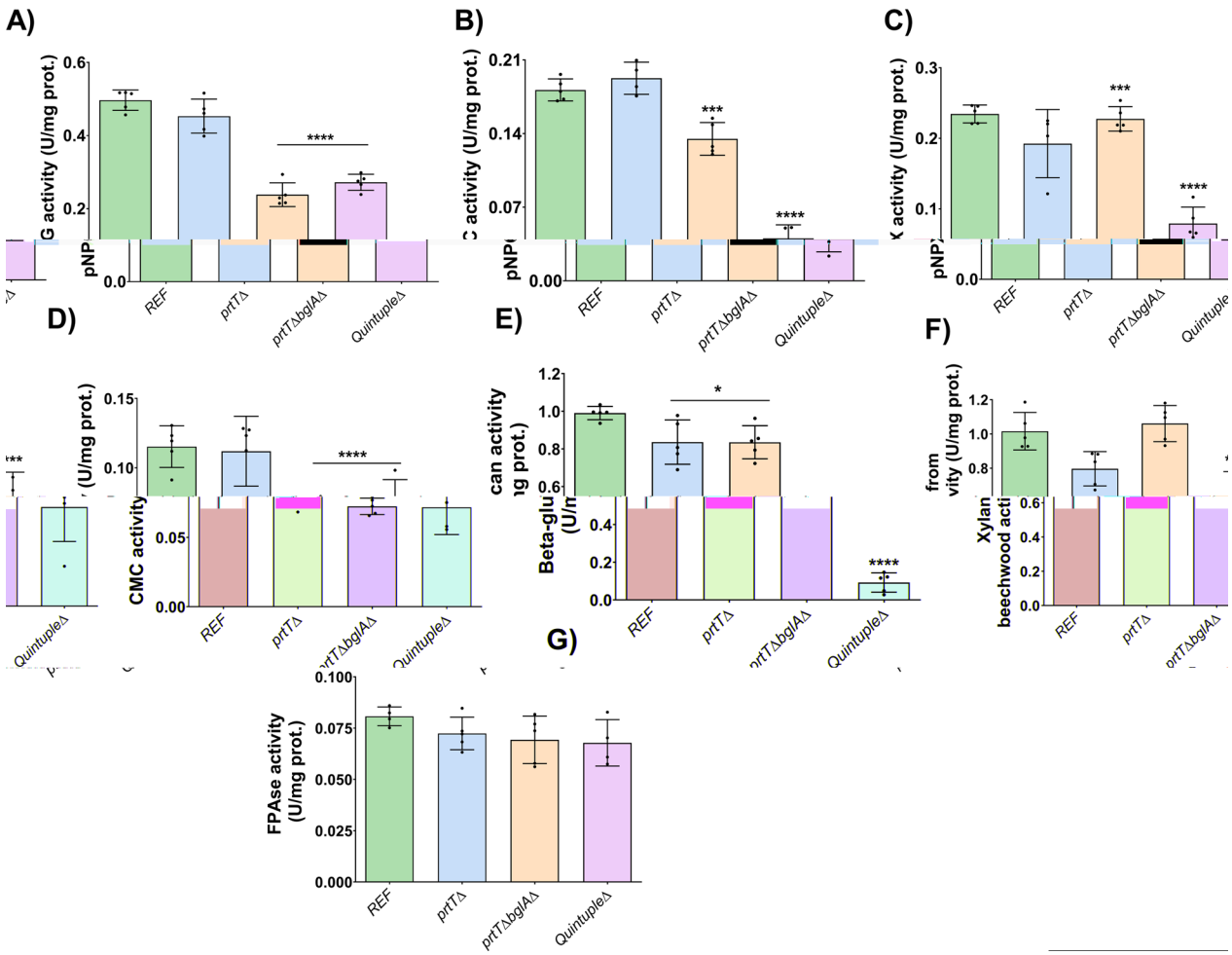

Fig. 2 Enzymatic activity profiles of the *REF*, *prtTΔ*, *prtTΔbglAΔ* and *QuintupleΔ* strains. Enzymatic activities (U/mg prot.) of the tailored strains secretomes using **A** pNPG, **B** pNPC, **C** pNPX, **D** CMC, **E** beta-glucan, **F** xylan from beechwood and **G** filter paper (FPase). Secretomes were produced using 1×10^6 spores/mL inoculated in a liquid medium supplemented with 1% (w/v) SCB for 72 h at 30 °C and 180 rpm. The experiment was conducted in five replicates. Statistical analysis was performed using multiple tests (two-factor ANOVA with Tukey's test—p-value ≤ 0.05) in comparison with the *REF* strain indicated as follows: *$p < 0.05$, **$p < 0.01$, ***$p < 0.001$

with the *prtTΔ* strain (Fig. 3B and C). Gluconic acid was produced by applying the *prtTΔ* and *prtTΔbglAΔ* secretomes (Fig. 3B). Xylobiose was detected only by using the *QuintupleΔ* secretome to digest SCS, while all secretomes released xylose (Fig. 3B). Comparison of *prtTΔ* vs *prtTΔbglAΔ* strains showed that deleting *bglA* drastically impacted glucose production from plant biomass (Fig. 3C). We then quantified biomass conversion and production of mono- and oligosaccharides. Secretome of the mutant strains produced a higher amount of COS, but the biomass conversion obtained with the *QuintupleΔ* secretome was reduced to about 50% (Fig. 3D). These data agree with previously published results showing that CBHs deletion in *Trichoderma reesei* decreases the efficiency of secretomes for plant biomass saccharification [57]. We found no statistical difference in glucan conversion between the Celluclast and *prtTΔ* secretome, corroborating that beta-glucosidases are the primary enzymes for glucose formation and increase glucan conversion [51, 60, 61] (Fig. 3D). In summary, a higher proportion of COS (cellobiose and cellotriose) was obtained using the secretome produced by *A. niger* tailored strain (*QuintupleΔ*) for plant biomass saccharification, but overall efficiency was reduced compared with the reference strain (*prtTΔ*).

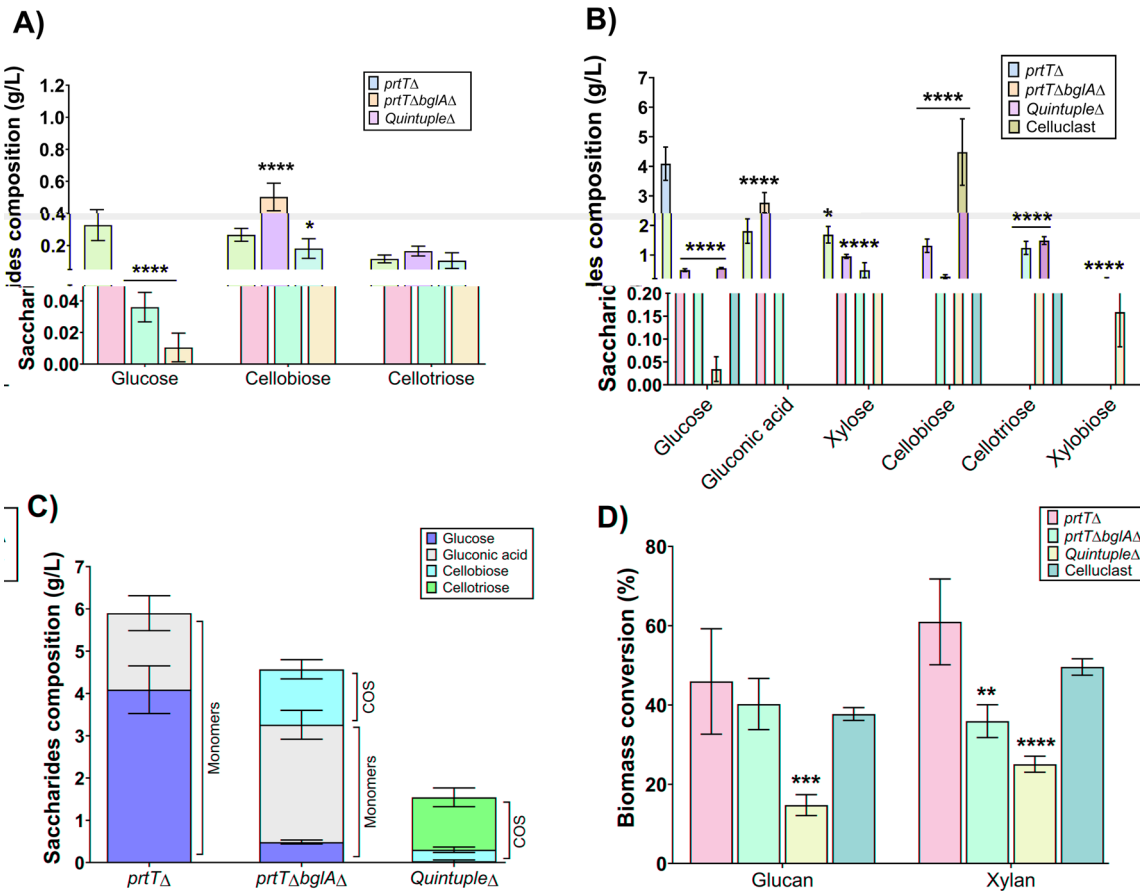

Fig. 3 Enzymatic saccharification of PASC and SCS by applying *prtTΔ*, *prtTΔbglAΔ* and *QuintupleΔ* secretomes. Quantitative analysis was performed using HPAEC-PAD to quantify mono- and oligosaccharides released from assays containing **A** PASC (0.5% w/v) for 24 h and **B** SCS (2% w/v) for 72 h. **C** Monomers and COS released from SCS assays. **D** Glucan and xylan conversion after 48 h. Assays were conducted using 20 µg of protein for PASC and 0.5 mg for SCS. Proteins were obtained from the secretomes of cultures containing 1×10^6 spores/mL inoculated in a liquid medium supplemented with 1% (w/v) of SCB for 72 h at 30 °C and 180 rpm. Protein amount applied for SCS assays was equivalent to 15 FPU/g Celluclast. PASC assays were performed in five replicates. SCS assays were performed in four replicates. Reactions containing 2% (w/v) solids loading in 50 mM sodium acetate pH 5.0 were incubated for 72 h at 50 °C and 1000 rpm. The data presented consists of mean values and standard deviations derived from biological replicates. Statistical analysis was performed using multiple tests (two-factor ANOVA with Tukey's test—p-value ≤ 0.05) in comparison with the *prtTΔ* indicated as follows: *$p < 0.05$, **$p < 0.01$, ***$p < 0.001$. Biomass conversion data were calculated stoichiometrically using the following anhydrous correction values: 0.90 for glucose, 0.95 for cellobiose, 0.96 for cellotriose, 0.83 for gluconic acid, 0.88 for xylose, and 0.94 for xylobiose

Deletion of additional *beta*-glucosidase genes in the *QuintupleΔ* strain does not further affect secretome activity

To investigate whether BGL activity in the secretome of tailored strains can be further reduced, alternative GH3 beta-glucosidase coding genes were deleted. *A. niger* genome has 19 putative genes encoding for BGLs (Additional Table 3), of which 11 contain signal peptides for secretion as predicted by the Signal P server [62]. Three genes were successfully deleted in the *Quintuple*Δ strain (Additional Tables 1 and 2), resulting in the *QuintupleΔASPNIDRAFT2_1099883Δ*, *QuintupleΔASPNIDRAFT2_1105418Δ*, and *QuintupleΔASPNIDRAFT2_1126962Δ* strains (Additional Table 1 and Additional Fig. 1D). The generated tailored strains presented similar amounts of secreted proteins (Additional Fig. 3A). No statistical differences were observed by comparing pNPG activity using the secretomes of *prtTΔbglAΔ*, *Quintuple*Δ, and the mutants with additional BGL deletions, indicating that *bglA* is the major BGL secreted by *A. niger* in the conditions evaluated (Additional Fig. 3B).

Elimination of exo-mode enzymes results in secretome rearrangement

To investigate how *A. niger* coped with the constraints from deleting genes coding significant enzymes involved in plant biomass degradation, the *prtTΔbglAΔ* and

*Quintuple*Δ secretomes produced on SCB were analyzed by MS. The *prtT*Δ, *prtT*Δ*bglA*Δ and *Quintuple*Δ secretomes contained 157, 146 and 152 proteins, respectively (and Fig. 4A and Additional Table 4). About 50% of the proteins identified in each secretome (76,73 and 71, respectively) were classified as CAZymes. Most CAZymes (69 proteins) were commonly present in all secretomes, and three were exclusively found in the *prtT*Δ secretome (Fig. 4B). Differential analysis of CAZymes (*prtT*Δ*bglA*Δ and *Quintuple*Δ relative to *prtT*Δ) revealed a GH105 upregulated exclusively in the *prtT*Δ*bglA*Δ, whereas 45 proteins were differently expressed only in the *Quintuple*Δ strain (Fig. 4C, D and Additional Table 4). Of the 45 differentially expressed proteins (DEPs) in the *Quintuple*Δ secretome, 30 were upregulated and 15 were downregulated (Fig. 4D). Thus, deleting multiple CAZymes affected the *Quintuple*Δ secretome drastically, suggesting a secretome rearrangement (Fig. 4D and Additional Table 4).

Differences in both secretomes were further investigated. A heatmap depicting the DEPs revealed that deletion and downregulation of the exoenzymes provide further evidence for the importance of BglA, CBHs, and XlnD in breaking down lignocellulosic biomass, as previously reported [41, 59, 60, 63, 64]. The tailored strains secreted alternative BGLs to compensate for the *bglA* deletion such as the ASPNIDRAFT2_1099883, an orthologue of the characterized *bglJ* from *A. oryzae* (Fig. 5 and Additional Table 4). *BglJ* shows high activity on synthetic substrates such as pNPG and cellobiose [65]. A second putative BGL was upregulated in the *QuintupleΔ* (ASPNIDRAFT2_1187703) secretome, an orthologue of *bgl3* from *A. oryzae* and *bglF* from *A. fumigatus* (Fig. 5 and Additional Table 4). These data suggest a compensation of BGL production when the most secreted enzyme (*BglA*) is knocked out (Additional Table 4).

Alternatively, the *QuintupleΔ* strain secreted two other CBHs (GH7) to compensate for the deletion of *cbhA* and *cbhB* (Fig. 5 and Additional Tables 3 and 4), indicating fungal plasticity. This suggests that those alternative CBHs were essential to maintain the cellulolytic capacity (Fig. 2G) and consequently sustain fungal growth in complex substrates such as SCB (Additional Fig. 2A). Moreover, the fungus remodels its secretome to explore other substrates besides cellulose. The *QuintupleΔ* strain also produced enzymes

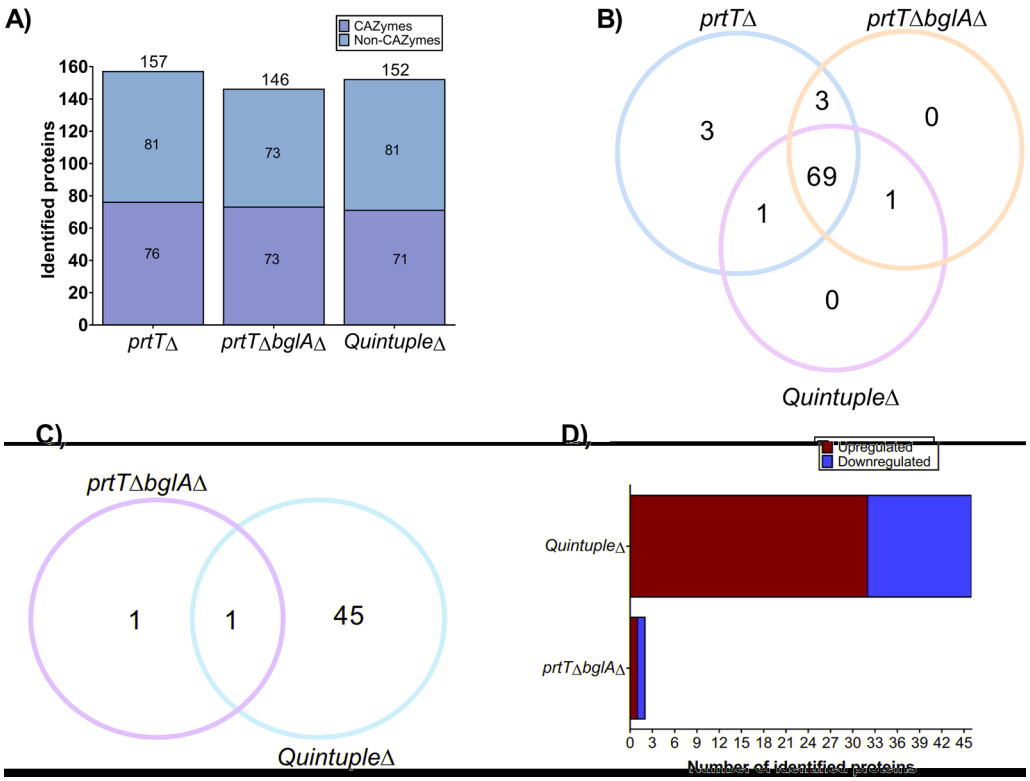

Fig. 4 *PrtT*Δ, *prtT*Δ*bglA*Δ and *Quintuple*Δ secretomes produced on SCB. **A** Number of proteins (CAZymes and Non-CAZymes) identified in the secretomes of tailored strains. Venn diagrams grouping **B** the CAZymes detected in the secretomes and **C** the differentially expressed proteins in *prtT*Δ*bglA*Δ and *Quintuple*Δ secretomes compared with *prtT*Δ. **D** Number of up- and downregulated CAZymes in the mutant strain secretomes

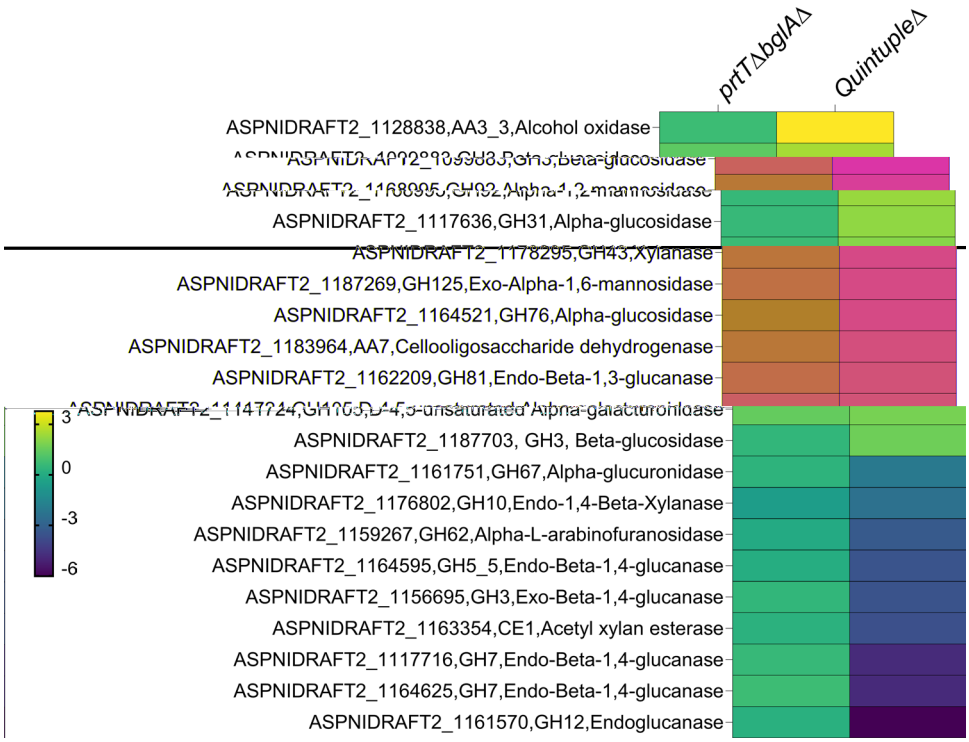

Fig. 5 Analysis of differentially expressed CAZymes in the *A. niger* tailored strains. Heatmap of the 20 differentially expressed CAZymes in the *A. niger* secretomes. Differential expression analysis was performed by applying log2 fold change ≤ 1 and ≥ − 1 and p-value ≤ 0.05 relative to *prtTΔ* strain

that break down minor polysaccharides in sugarcane biomass, including a GH31 (ASPNIDRAFT2_1117636) and GH76 (ASPNIDRAFT2_1164521) involved in xyloglucan metabolism, and arabinofuranosidase (ASPNIDRAFT2_1159267) and xylanases (GH10 and GH43, ASPNIDRAFT2_1176802 and ASPNIDRAFT2_1,178,295) involved in hemicellulose metabolism (Fig. 5 and Additional Table 4). In this regard, the *prtTΔbglAΔ* strain abundantly secreted ASPNIDRAFT2_1141724, a predicted GH105 involved in pectin degradation [66, 67] (Fig. 5 and Additional Table 4). Minor plant biomass components can provide energy for *A. niger* growth in the absence of critical cellulases. Similar results were obtained in *A. niger* by deleting genes encoding transcription factors involved in (hemi)cellulose metabolism [63], revealing a flexible regulatory system that can facilitate the use of most plant biomass components [63]. Additionally, enzymes such as mannosidases (ASPNIDRAFT2_1168995 and ASPNIDRAFT2_1187269), glucosidases (ASPNIDRAFT2_1164521 and ASPNIDRAFT2_1117636) and oxidases (ASPNIDRAFT2_1128838 and ASPNIDRAFT2_1183964) were also found in *QuintupleΔ* strain heatmap (Fig. 5 and Additional Table 4). These enzymes are usually secreted in oxidative stress and/or starvation, generating inducers from complex substrates [68–71]. Importantly, cellobiose and cellotriose transporters were identified in *A. niger*, such as *CtA* [72]. All this evidence may also explain the tailored strains' effective growth despite the absence of major CBHs and BGLs.

Conclusion

The *A. niger* secretome produced on a lignocellulosic substrate was engineered to design a tailored enzyme cocktail for partial lignocellulose degradation. Application of *A. niger* tailored strain secretomes for sugarcane biomass degradation resulted in a higher COS/glucose ratio, showing that deleting some enzymatic components is an efficient approach. Fungal plasticity was demonstrated as alternative cellulases were secreted in addition to enzymes targeting minor components of plant cell wall, which was an efficient strategy to sustain fungal growth in plant biomass. The lack of impairment in fungal growth on plant biomass suggests that tailored strains uptake COS as a carbon source. Thus, exoenzyme deletion is a promising approach to obtaining tailored enzymatic cocktails for oligosaccharide production from plant biomass. Our findings provide insight into the remarkable adaptability of fungi and their ability to thrive under diverse conditions.

Supplementary Information

The online version contains supplementary material available at https://doi.org/10.1186/s12934-024-02578-9.

Supplementary Material 1.

Supplementary Material 2. Additional Figure 1. Confirmation of gene deletions for the tailored *prtTΔ*, *prtTΔbglAΔ*, *QuintupleΔ* and *QuintupleΔ* strains containing the deletion of additional beta-glucosidases. Agarose gels (1%) were used for PCR diagnostic tests using genomic DNA from *REF* and tailored strains. These tests were conducted to confirm the deletion of (A) extracellular protease regulator (*prtT*), (B) the four main CAZymes (*cbhA*, *cbhB*, *bglA*, and *xlnD*) and *prtT*, (C) beta-glucosidase A (*bglA*), and (D) the additional beta-glucosidases. *QΔ*: *QuintupleΔ*. MW: Molecular Weight.

Supplementary Material 3. Additional Figure 2. Phenotypic analysis of the *prtTΔ*, *prtTΔbglAΔ* and *QuintupleΔ* strains. (A) Cultivation of tailored strains on agar minimal medium (MM) plates supplemented with 1% (w/v) of glucose, Avicel, carboxymethyl cellulose (CMC), hydrothermally and deacetylated pretreated sugarcane bagasse (SCB), xylan from beechwood and xylose. A total of 1×10^5 spores were inoculated in the center of the plates and maintained at 30 ºC for 7 days. (B) SDS-PAGE gels (12%) showing the protein secretion profiles (secretomes) of *REF* and tailored strains. Red arrows represent the absent bands in the *QuintupleΔ* strain. Secretomes were obtained from cultures containing 1×10^6 spores/mL inoculated in a liquid medium supplemented with 1% (w/v) SCB for 72 h at 30 °C and 180 rpm. Cultivation was conducted in five replicates. MW: Molecular Weight.

Supplementary Material 4. Additional Figure 3. Characterization of the *A. niger* mutant strains with deletion of additional beta-glucosidases. (A) Protein amount (mg/mL) in the secretomes. (B) Enzymatic activity (U/mg prot.) of secretomes using pNPG as substrate. Cultivation (4 biological replicates) was performed in a liquid medium supplemented with 1% (w/v) SCB for 72 h at 30 °C and 180 rpm. Statistical analysis was performed using multiple tests (two-factor ANOVA with Tukey's test – p-value ≤0.05) in comparison with the *prtTΔ* strain.

Acknowledgements
The authors thank DTU Proteomics Core for MS analysis. Special thanks to the multi-user facility (EMU) at IB/UNICAMP (FAPESP 20/05784-3) and Espaço da Escrita - Pró-Reitoria de Pesquisa – UNICAMP for the language services provided. We also thank Victor Corasolla Carregari and Bradley Smith from the Laboratory of Neuroproteomics (LNP/IB/UNICAMP) for assistance with MS data analysis and Paulo A. Baldasso and Aryadne Gasparini Rodrigues for technical assistance.

Author contributions
FLF and FJC designed and performed main experiments, analyzed data and wrote the manuscript. CRFT contributed to experiments involving plant biomass saccharification, ergosterol analysis and wrote the manuscript. ABC contributed to experiments involving fungal growth and enzymatic activity. JAG, NSW and EPA contributed to gene deletions and tailored strains validations. LL contributed to proteomics data analysis. SCR performed mass balance and calculations. TTF provided resources. AD and UHM supervised the project and revised the final version of the manuscript. All authors read and approved the final manuscript.

Funding
FLF and FJC were funded by FAPESP (São Paulo Research Foundation 19/21609-0, 17/26370-0 and 17/10083-1, respectively). CRFT, JAG, NWS and EPA received FAPESP fellowships. AD was supported by FAPESP grants 15/50612-8 and 22/05731-2.

Availability of data and materials
Data is provided within the manuscript or supplementary information files. The secretome raw data, withthe identifier MSV000095310, is available from MassIVE Repository. A detailed guide for the proteomic analysis can be also found in the GitHub repository (https://github.com/hiyama341/KO-of-exoce llulases).

Declarations

Competing interests
The authors declare no competing interests.

Author details
[1]Laboratory of Enzymology and Molecular Biology of Microorganisms (LEBIMO), Department of Biochemistry and Tissue Biology, Institute of Biology, Universidade Estadual de Campinas (UNICAMP), Campinas, SP 13083-862, Brazil. [2]Department of Biotechnology and Biomedicine, Technical University of Denmark (DTU), Søltofts Plads, Building 223, Kongens Lyngby, 2800, Denmark. [3]Department of Bioprocess and Biotechnology, School of Agricultural Sciences, São Paulo State University (UNESP), Botucatu, SP, Brazil. [4]Interdisciplinary Center of Energy Planning, Universidade Estadual de Campinas (UNICAMP), Campinas, SP 13083-862, Brazil.

Received: 10 July 2024 Accepted: 2 November 2024
Published online: 29 November 2024

References

1. Junqueira TL, Chagas MF, Gouveia VLR, Rezende MCAF, Watanabe MDB, Jesus CDF, et al. Techno-economic analysis and climate change impacts of sugarcane biorefineries considering different time horizons. Biotechnol Biofuels. 2017;10:1–12.
2. Islam MK, Wang H, Rehman S, Dong C, Hsu HY, Lin CSK, et al. Sustainability metrics of pretreatment processes in a waste derived lignocellulosic biomass biorefinery. Bioresour Technol. 2020;298: 122558.
3. Gustavsson L, Holmberg J, Dornburg V, Sathre R, Eggers T, Mahapatra K, et al. Using biomass for climate change mitigation and oil use reduction. Energy Policy. 2007;35:5671–91.
4. Cherubini F. The biorefinery concept: using biomass instead of oil for producing energy and chemicals. Energy Convers Manag. 2010;51:1412–21.
5. Fernandes BS, Vieira JPF, Contesini FJ, Mantelatto PE, Zaiat M, da Pradella JG. High value added lipids produced by microorganisms: a potential use of sugarcane vinasse. Crit Rev Biotechnol. 2017;37:1048–61.
6. Chuaboon L, Wongnate T, Punthong P, Kiattisewee C, Lawan N, Hsu CY, et al. One-pot bioconversion of l-Arabinose to l-ribulose in an enzymatic cascade. Angew Chemie - Int Ed. 2019;58:2428–32.
7. Özdenkçi K, De Blasio C, Muddassar HR, Melin K, Oinas P, Koskinen J, et al. A novel biorefinery integration concept for lignocellulosic biomass. Energy Convers Manag. 2017;149:974–87.
8. Modig T, Almeida JRM, Gorwa-Grauslund MF, Lidén G. Variability of the response of *Saccharomyces cerevisiae* strains to lignocellulose hydrolysate. Biotechnol Bioeng. 2008;100:423–9.
9. Li H, Shen Y, Wu M, Hou J, Jiao C, Li Z, et al. Engineering a wild-type diploid *Saccharomyces cerevisiae* strain for second-generation bioethanol production. Bioresour Bioprocess. 2016.
10. Shin HD, Yoon SH, Wu J, Rutter C, Kim SW, Chen RR. High-yield production of meso-2,3-butanediol from cellodextrin by engineered *E. coli* biocatalysts. Bioresour Technol. 2012;118:367–73.
11. Barbosa FC, Kendrick E, Brenelli LB, Arruda HS, Pastore GM, Rabelo SC, et al. Optimization of cello-oligosaccharides production by enzymatic hydrolysis of hydrothermally pretreated sugarcane straw using cellulolytic and oxidative enzymes. Biomass Bioenergy. 2020;141: 105697.
12. Chen R. A paradigm shift in biomass technology from complete to partial cellulose hydrolysis: lessons learned from nature. Bioengineered. 2015;6:69–72.
13. Xu J-L, Liu Z-F, Zhang X-W, Liu H-L, Wang Y. Microbial oligosaccharides with biomedical applications. Mar Drugs. 2021;19:350.
14. Mussatto SI, Mancilha IM. Non-digestible oligosaccharides: a review. Carbohydr Polym. 2007;68:587–97.
15. Rastall RA. Functional oligosaccharides: application and manufacture. Annu Rev Food Sci Technol. 2010;1:305–39.
16. Karnaouri A, Matsakas L, Krikigianni E, Rova U, Christakopoulos P. Valorization of waste forest biomass toward the production of cello-oligosaccharides with potential prebiotic activity by utilizing customized enzyme cocktails. Biotechnol Biofuels. 2019;12:285.

17. Forsan CF, de Freitas C, Brienzo M. Cello-oligosaccharides and xylooligosaccharides production by a combination of mechanical, chemical, and enzymatic treatments of banana pseudostem and leaves and guava bagasse. BioEnergy Res. 2023;17:129–44.
18. Zhong C, Ukowitz C, Domig KJ, Nidetzky B. Short-chain cello-oligosaccharides: intensification and scale-up of their enzymatic production and selective growth promotion among probiotic bacteria. J Agric Food Chem. 2020;68:8557–67.
19. Nogueira KMV, Mendes V, Carraro CB, Taveira IC, Oshiquiri LH, Gupta VK, et al. Sugar transporters from industrial fungi: key to improving second-generation ethanol production. Renew Sustain Energy Rev. 2020;131: 109991.
20. Damon C, Vallon L, Zimmermann S, Haider MZ, Galeote V, Dequin S, et al. A novel fungal family of oligopeptide transporters identified by functional metatranscriptomics of soil eukaryotes. ISME J. 2011;5:1871–80.
21. Fang W, St. Leger RJ. Mrt, a gene unique to fungi, encodes an oligosaccharide transporter and facilitates rhizosphere competency in *Metarhizium robertsii*. Plant Physiol. 2010;154:1549–57.
22. Brenelli LB, Figueiredo FL, Damasio A, Franco TT, Rabelo SC. An integrated approach to obtain xylo-oligosaccharides from sugarcane straw: from lab to pilot scale. Bioresour Technol. 2020;313: 123637.
23. Barbosa FC, Franco TT, David LB. Production of cello-oligosaccharides through the biorefinery concept: a technical-economic and life-cycle assessment. Biofuels, Bioprod Bioref. 2021;15:1763–74.
24. Eibinger M, Ganner T, Bubner P, Rošker S, Kracher D, Haltrich D, et al. Cellulose surface degradation by a lytic polysaccharide monooxygenase and its effect on cellulase hydrolytic efficiency. J Biol Chem. 2014;289:35929–38.
25. Quinlan RJ, Sweeney MD, Lo Leggio L, Otten H, Poulsen JCN, Johansen KS, et al. Insights into the oxidative degradation of cellulose by a copper metalloenzyme that exploits biomass components. Proc Natl Acad Sci USA. 2011;108:15079–84.
26. Abe K, Gomi K, Hasegawa F, Machida M. Impact of *Aspergillus oryzae* genomics on industrial production of metabolites. Mycopathologia. 2006;162:143–53.
27. Song B, Li B, Wang X, Shen W, Park S, Collings C, et al. Real-time imaging reveals that lytic polysaccharide monooxygenase promotes cellulase activity by increasing cellulose accessibility. Biotechnol Biofuels. 2018;11:1–11.
28. Ávila PF, Goldbeck R. Fractionating process of lignocellulosic biomass for the enzymatic production of short chain cello-oligosaccharides. Ind Crops Prod. 2022;178: 114671.
29. Ávila PF, Silva MF, Martins M, Goldbeck R. Cello-oligosaccharides production from lignocellulosic biomass and their emerging prebiotic applications. World J Microbiol Biotechnol. 2021;37:73.
30. Liang X, Yoshida T, Uryu T. Direct saccharification and ethanol fermentation of cello-oligosaccharides with recombinant yeast. Carbohydr Polym. 2013;91:157–61.
31. Okabe M, Lies D, Kanamasa S, Park EY. Biotechnological production of itaconic acid and its biosynthesis in *Aspergillus terreus*. Appl Microbiol Biotechnol. 2009;84:597–606.
32. Cairns TC, Nai C, Meyer V. How a fungus shapes biotechnology: 100 years of *Aspergillus niger* research. Fungal Biol Biotechnol. 2018;5:1–14.
33. Garrigues S, Kun RS, de Vries RP. Genetic barcodes allow traceability of CRISPR/Cas9-derived *Aspergillus niger* strains without affecting their fitness. Curr Genet. 2021;67:673–84.
34. Nødvig CS, Nielsen JB, Kogle ME, Mortensen UH. A CRISPR-Cas9 system for genetic engineering of filamentous fungi. PLoS ONE. 2015;10: e0133085.
35. Fiedler MRM, Barthel L, Kubisch C, Nai C, Meyer V. Construction of an improved *Aspergillus niger* platform for enhanced glucoamylase secretion. Microb Cell Fact. 2018;17:1–12.
36. Zubieta MP, Gerhardt JA, Rubio MV, Terrasan CRF, Persinoti GF, Antoniel EP, et al. Improvement of homologous GH10 xylanase production by deletion of genes with predicted function in the *Aspergillus nidulans* secretion pathway. Microb Biotechnol. 2020;13:1245–53.
37. Sui YF, Schütze T, Ouyang LM, Lu H, Liu P, Xiao X, et al. Engineering cofactor metabolism for improved protein and glucoamylase production in *Aspergillus niger*. Microb Cell Fact. 2020;19:1–17.
38. Zhang H, Wang S, Zhang X, Ji W, Song F, Zhao Y, et al. The amyR-deletion strain of *Aspergillus niger* CICC2462 is a suitable host strain to express secreted protein with a low background. Microb Cell Fact. 2016;15:68.
39. Kamaruddin N, Storms R, Mahadi NM, Illias RM, Bakar FDA, Murad AMA. Reduction of extracellular proteases increased activity and stability of heterologous protein in *Aspergillus niger*. Arab J Sci Eng. 2018;43:3327–38.
40. Chylenski P, Forsberg Z, Ståhlberg J, Várnai A, Lersch M, Bengtsson O, et al. Development of minimal enzyme cocktails for hydrolysis of sulfite-pulped lignocellulosic biomass. J Biotechnol. 2017;246:16–23.
41. Borin GP, Sanchez CC, de Pereira Souza A, de Silva Santana E, de Tieppo Souza A, Franco A, et al. Comparative secretome analysis of *Trichoderma reesei* and *Aspergillus niger* during growth on sugarcane biomass. PLoS ONE. 2015;10(6): e0129275.
42. Stajich JE, Harris T, Brunk BP, Brestelli J, Fischer S, Harb OS, et al. FungiDB: an integrated functional genomics database for fungi. Nucleic Acids Res. 2012;40: D675.
43. Grigoriev IV, Nikitin R, Haridas S, Kuo A, Ohm R, Otillar R, et al. MycoCosm portal: gearing up for 1000 fungal genomes. Nucleic Acids Res. 2014;42: D699.
44. Nørholm MH. A mutant Pfu DNA polymerase designed for advanced uracil-excision DNA engineering. BMC Biotechnol. 2010;10:21.
45. Nour-Eldin HH, Geu-Flores F, Halkier BA. USER cloning and USER fusion: the ideal cloning techniques for small and big laboratories. Methods Mol Biol. 2010;643:185–200.
46. Nødvig CS, Hoof JB, Kogle ME, Jarczynska ZD, Lehmbeck J, Klitgaard DK, et al. Efficient oligo nucleotide mediated CRISPR-Cas9 gene editing in Aspergilli. Fungal Genet Biol. 2018;115:78–89.
47. Hansen BG, Salomonsen B, Nielsen MT, Nielsen JB, Hansen NB, Nielsen KF, et al. Versatile enzyme expression and characterization system for *Aspergillus nidulans*, with the *Penicillium brevicompactum* polyketide synthase gene from the mycophenolic acid gene cluster as a test case. Appl Environ Microbiol. 2011;77:3044–51.
48. Nielsen ML, Albertsen L, Lettier G, Nielsen JB, Mortensen UH. Efficient PCR-based gene targeting with a recyclable marker for *Aspergillus nidulans*. Fungal Genet Biol. 2006;43:54–64.
49. Laemmli UK. Cleavage of structural proteins during the assembly of the head of bacteriophage T4. Nature. 1970;227:680–5.
50. Terrasan CRF, Rubio MV, Gerhardt JA, Cairo JPF, Contesini FJ, Zubieta MP, et al. Deletion of AA9 lytic polysaccharide monooxygenases impacts *A. nidulans* secretome and growth on lignocellulose. Microbiol Spectr. 2022;10:e02125-e2221.
51. Decker SR, Adney WS, Jennings E, Vinzant TB, Himmel ME. Automated filter paper assay for determination of cellulase activity. Appl Biochem Biotechnol. 2003;107:689–704.
52. Miller GL. Use of dinitrosalicylic acid reagent for determination of reducing sugar. Anal Chem. 1959;31:426–8.
53. Wood TM, Bhat KM. Methods for measuring cellulase activities. Methods Enzymol. Academic Press; 1988. p. 87–112.
54. Xu Y, Fan L, Wang X, Yong Q, Yu S-Y. Simultaneous separation and quantification of linear xylo- and cello-oligosaccharides mixtures in lignocellulosics processing products on high-performance anion-exchange chromatography coupled with pulsed amperometric detection. BioResources. 2013;8:3247–59.
55. Basenko EY, Pulman JA, Shanmugasundram A, Harb OS, Crouch K, Starns D, et al. FungiDB: an integrated bioinformatic resource for fungi and oomycetes. J Fungi. 2018;4:39.
56. Zhu L, Maruyama JI, Kitamoto K. Further enhanced production of heterologous proteins by double-gene disruption (ΔAosedD Δaovps10) in a hyper-producing mutant of *Aspergillus oryzae*. Appl Microbiol Biotechnol. 2013;97:6347–57.
57. Zoglowek M, Lübeck PS, Ahring BK, Lübeck M. Heterologous expression of cellobiohydrolases in filamentous fungi - an update on the current challenges, achievements and perspectives. Process Biochem. 2015;50:211–20.
58. Busk PK, Lange M, Pilgaard B, Lange L. Several genes encoding enzymes with the same activity are necessary for aerobic fungal degradation of cellulose in nature. PLoS ONE. 2014;9: e114138.
59. Rodrigues AC, Haven MØ, Lindedam J, Felby C, Gama M. Celluclast and Cellic® CTec2: saccharification/fermentation of wheat straw, solid–liquid partition and potential of enzyme recycling by alkaline washing. Enzyme Microb Technol. 2015;79–80:70–7.

60. Ren M, Wang Y, Liu G, Zuo B, Zhang Y, Wang Y, et al. The effects of deletion of cellobiohydrolase genes on carbon source-dependent growth and enzymatic lignocellulose hydrolysis in *Trichoderma reesei*. J Microbiol. 2020;58:687–95.
61. Lemos MA, Teixeira JA, Domingues MRM, Mota M, Gama FM. The enhancement of the cellulolytic activity of cellobiohydrolase I and endoglucanase by the addition of cellulose binding domains derived from *Trichoderma reesei*. Enzyme Microb Technol. 2003;32:35–40.
62. Petersen TN, Brunak S, von Heijne G, Nielsen H. SignalP 4.0: discriminating signal peptides from transmembrane regions. Nat Methods. 2011;8:785–6.
63. Kun RS, Garrigues S, Di Falco M, Tsang A, de Vries RP. Blocking utilization of major plant biomass polysaccharides leads *Aspergillus niger* towards utilization of minor components. Microb Biotechnol. 2021;14:1683–98.
64. Mattam AJ, Chaudhari YB, Velankar HR. Factors regulating cellulolytic gene expression in filamentous fungi: an overview. Microb Cell Fact. 2022;21:44.
65. Kudo K, Watanabe A, Ujiie S, Shintani T, Gomi K. Purification and enzymatic characterization of secretory glycoside hydrolase family 3 (GH3) aryl β-glucosidases screened from *Aspergillus oryzae* genome. J Biosci Bioeng. 2015;120:614–23.
66. Schmitt CC, Moreira R, Neves RC, Richter D, Funke A, Raffelt K, et al. From agriculture residue to upgraded product: the thermochemical conversion of sugarcane bagasse for fuel and chemical products. Fuel Process Technol. 2020;197: 106199.
67. Alazi E, Niu J, Kowalczyk JE, Peng M, Aguilar Pontes MV, van Kan JAL, et al. The transcriptional activator GaaR of *Aspergillus niger* is required for release and utilization of d-galacturonic acid from pectin. FEBS Lett. 2016;590:1804–15.
68. van Munster JM, Daly P, Delmas S, Pullan ST, Blythe MJ, Malla S, et al. The role of carbon starvation in the induction of enzymes that degrade plant-derived carbohydrates in *Aspergillus niger*. Fungal Genet Biol. 2014;72:34–47.
69. Aguirre J, Hansberg W, Navarro R. Fungal responses to reactive oxygen species. Med Mycol. 2006;44:101–7.
70. Nitsche BM, Jørgensen TR, Akeroyd M, Meyer V, Ram AF. The carbon starvation response of *Aspergillus niger* during submerged cultivation: insights from the transcriptome and secretome. BMC Genomics. 2012;13:380.
71. Meyer V, Fiedler M, Nitsche B, King R. The cell factory Aspergillus enters the big data era: opportunities and challenges for optimising product formation. 2015;91–132.
72. Lin H, Zhao J, Zhang Q, Cui S, Fan Z, Chen H, et al. Identification and characterization of a cellodextrin transporter in *Aspergillus niger*. Front Microbiol. 2020;11:145.

Publisher's Note